JACS
JOURNAL OF THE AMERICAN CHEMICAL SOCIETY
Article
pubs.acs.org/JACS

Photoswitching Azo Compounds in Vivo with Red Light

Subhas Samanta,[†,§] Andrew A. Beharry,[†,§] Oleg Sadovski,[†] Theresa M. McCormick,[†] Amirhossein Babalhavaeji,[†] Vince Tropepe,[‡] and G. Andrew Woolley*[,†]

[†]Department of Chemistry, University of Toronto, 80 St. George Street, Toronto, Ontario M5S 3H6, Canada

[‡]Department of Cell and Systems Biology and Centre for the Analysis of Genome Evolution and Function, University of Toronto, 25 Harbord Street, Toronto, Ontario M5S 3G5, Canada

Supporting Information

ABSTRACT: The photoisomerization of azobenzenes provides a general means for the photocontrol of molecular structure and function. For applications in vivo, however, the wavelength of irradiation required for trans-to-cis isomerization of azobenzenes is critical since UV and most visible wavelengths are strongly scattered by cells and tissues. We report here that azobenzene compounds in which all four positions ortho to the azo group are substituted with bulky electron-rich substituents can be effectively isomerized with red light (630−660 nm), a wavelength range that is orders of magnitude more penetrating through tissue than other parts of the visible spectrum. When the ortho substituent is chloro, the compounds also exhibit stability to reduction by glutathione, enabling their use in intracellular environments in vivo.

INTRODUCTION

Photochemical switches are broadly useful tools; they permit one to use a highly versatile reagent, light, to direct molecular responses in a reversible (on/off) manner. A number of molecular classes are known to undergo photoisomerization.[1] The majority of these, however, require UV light for at least one of the photoswitching directions. Except in certain model organisms, such as *C. elegans* and the zebrafish,[2] and in specialized organs such as the eye, in vivo single-photon optical applications require red (or near-infrared) light to achieve significant penetration through tissue.[3] Naturally occurring photoswitches such as the phytochromes and the rhodopsins have evolved to undergo red-light photochemistry, and several of these are being engineered as tools for manipulating molecular processes in vivo.[4,5] These photoswitches are limited to protein photocontrol, however, and their requirement for large protein cofactors limits versatility for nanotechnology applications.

The photoisomerization of azobenzene, discovered in 1937,[6] is a well-defined and extensively applied process. The parent molecule is approximately planar in its thermally stable trans conformation. Irradiation with UV light produces the cis isomer, which has a bent conformation and a much larger dipole moment. These molecular changes have been used to drive a myriad of functional outcomes in various settings.[7,8] While application of azo compounds in living cells and tissues has been achieved in specific cases,[2,9−14] the limitations of using UV light in vivo have driven efforts to prepare azo compound that operate with longer wavelengths of light.[15,16]

Previously we found that the tetra-ortho-methoxy-substituted azobenzene derivative (**1-rf**) has n−π^* transitions in the visible (blue/green) region that are well separated for the cis and trans isomers making photochemical switching possible without using UV light.[17] Unlike derivatives in which the $\pi-\pi^*$ transitions are shifted to longer wavelengths,[18,19] these ortho-substituted species showed slow (hours) thermal back reactions.

C2-bridged azobenzene species have also been reported that have well-separated n−π^* transitions and can be isomerized with visible light.[20−22] In these cases, however, the trans isomer, which has the longer-wavelength absorption band, is thermodynamically less stable than the cis isomer. Control of molecular processes in settings where only long-wavelength light can penetrate may be easier to achieve if light drives production of the thermodynamically less stable isomer and the system relaxes thermally in the dark.

Recently Aprahamian and colleagues[23] and Hecht and colleagues[24] have reported that BF_2-coordinated azobenzenes and ortho-fluoro-substituted azobenzenes, respectively, can also exhibit visible light switching properties. Since visible light switching is appealing for use in biological systems that are sensitive to UV light, we decided to explore more fully the behavior of this type of photoswitch. We report the discovery that a variety of tetra-ortho-substituted azobenzene compounds can be effectively isomerized with red light (see Chart 1). In addition, ortho-chloro-substitution confers stability to reduction by glutathione enabling use of these switches in intracellular environments in vivo.

MATERIALS AND METHODS

Synthetic Methods. The compound **1-rf** was prepared previously.[17] The route employed in that case proved difficult to adapt to the synthesis of a chloroacetamido-substituted version (**1**)

Received: March 10, 2013
Published: June 10, 2013

   dx.doi.org/10.1021/ja402220t | J. Am. Chem. Soc. 2013, 135, 9777−9784

Chart 1. Tetra-Ortho-Substituted Azobenzene Derivatives Studied Here

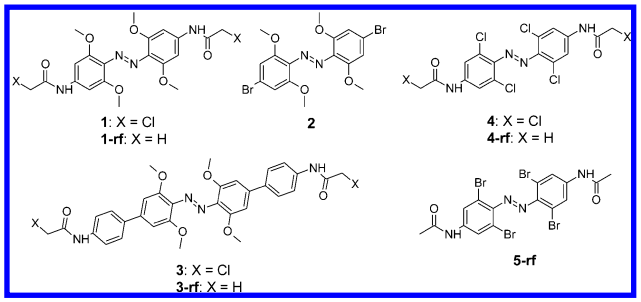

suitable for cross-linking to peptides. Instead we adopted the synthetic route shown in Scheme 1.

Scheme 1. Synthesis of 1[a]

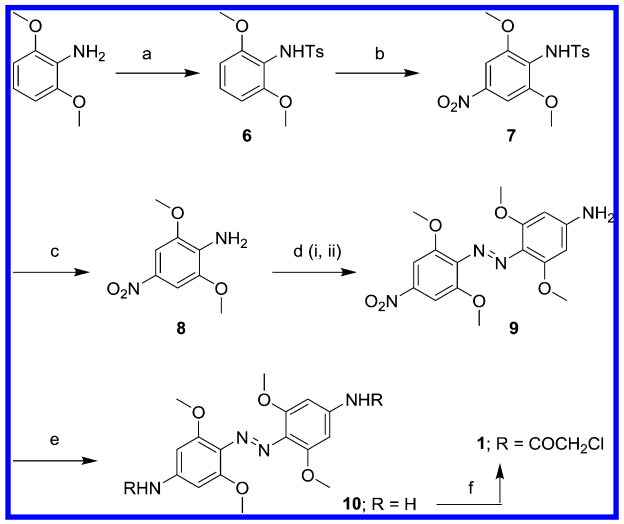

[a]Conditions and reagents: (a) *p*-Toluenesulfonyl chloride, pyridine, 100 °C, 1 h, yield 80%; (b) $NaNO_2$, HNO_3/AcOH, yield 60%; (c) Conc. H_2SO_4, 16 h, yield 70%; (d) i) $NaNO_2$, dil. HCl, 0−5 °C, 20 min ii) 3,5-dimethoxyaniline, H_2O, sat. $NaHCO_3$ (pH 8−9), 5 °C to rt, 12 h, yield 31%; (e) $SnCl_2$, anhyd. DMSO, 48 h, yield 7%; (f) chloroacetyl chloride, triethylamine, $CHCl_3$, 5 °C to rt, 12 h, yield 62%.

This approach makes use of the para-directing property of the tosyl group under the specific reaction conditions to cleanly give **7** as originally noted by Wepster.[25] Reduction of **9** to give **10** gave low yields likely for the same reasons that the final compound is sensitive to reduction by glutathione (vide infra).

The syntheses of **3** and **3-rf** were achieved as shown in Scheme 2. In this case a reductive step was avoided; the azo unit was formed using potassium permanganate and copper sulfate[26] and elaborated using a Suzuki reaction to give **13**. Initial nitration of 1-bromo-3,5-dimethoxybenzene led to the production of two isomers. The major product was 1-bromo-3,5-dimethoxy-2-nitrobenzene. The production of **2** using $KMnO_4$−$CuSO_4{\cdot}5H_2O$ was successful, but the yield was low; a highly polar side product was formed, which we could not characterize. The yields of Suzuki cross-coupling reactions were also comparatively low. Even though we used nearly 3−4 equiv of arylboronic acids and long reaction times, significant amounts of mono-coupled products were isolated. Yields of the bis-coupled products might be improved by systematic testing of different solvents and reaction conditions.

Syntheses of the tetra-ortho-halo derivatives (**4**, **4-rf**, and **5-rf**) are outlined in Scheme 3. AgO oxidation of commercially available 4-acetamido-2,6-dibromoaniline led to **5-rf** in only 10% yield and several

Scheme 2. Synthesis of 3 and 3-rf[a]

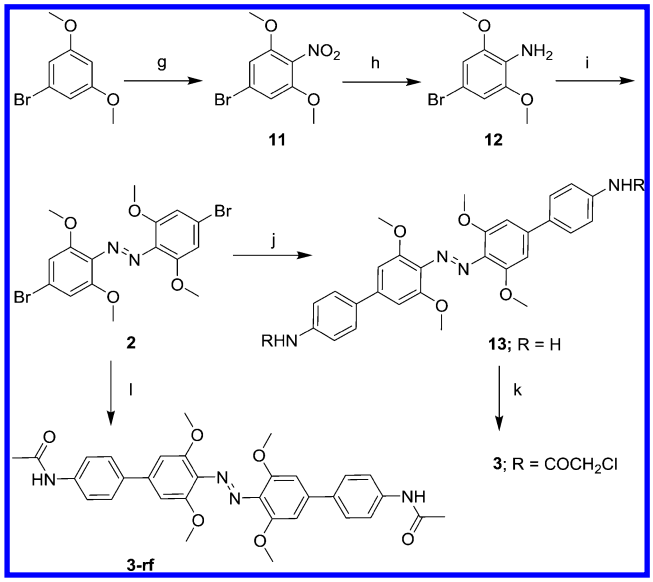

[a](g) HNO_3, Ac_2O, 0 °C to rt, 4 h, yield 19%; (h) Fe, NH_4Cl, MeOH, reflux 4 h, yield 57%; (i) $KMnO_4$−$CuSO_4{\cdot}5H_2O$, dichloromethane, reflux, 48 h, yield 20%; (j) 4-aminophenylboronic acid hydrochloride, $Pd(PPh_3)_4$, $NaHCO_3$, anhyd. 1,2-dimethoxyethane, 90 °C, 24 h, yield 54%; (k) chloroacetyl chloride, K_2CO_3, anhyd. DMF, 0 °C−rt, 3 h, yield 62%; (l) 4-acetamidophenylboronic acid, $Pd(PPh_3)_4$, K_2CO_3, anhyd. 1,4-dioxane, 110 °C, 24 h, yield 33%.

Scheme 3. Synthesis of 4, 4-rf, and 5[a]

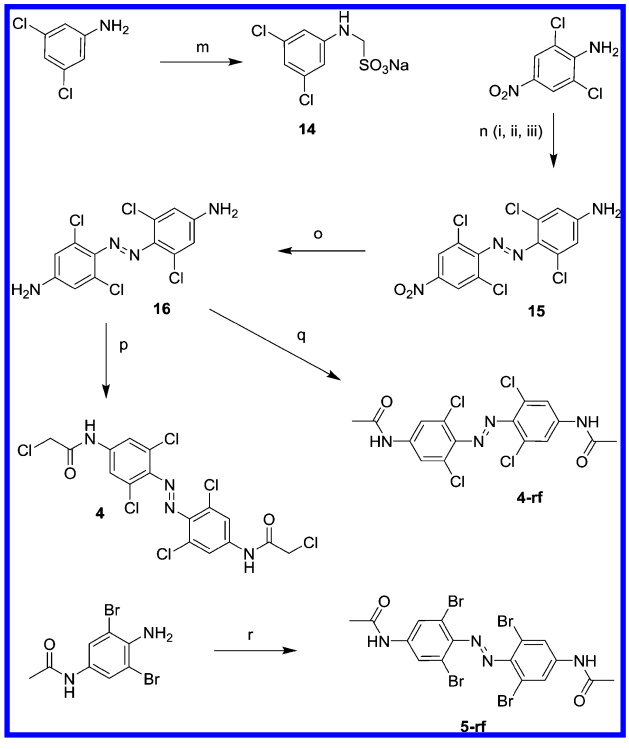

[a](m) HCHO, $NaHSO_3$, EtOH/H_2O, 70 °C, 24 h, yield 84%; (n) i) $NaNO_2$, H_2SO_4, AcOH/DMF, 0° C, 2 h, ii) **14**, DMF, 0 °C to rt, 72 h, iii) 20% NaOH, 70 °C, 2 h, overall yield 26%; (o) Na_2S, 1,4-dioxane/EtOH/H_2O, 90 °C, 24 h, yield 42%; (p) chloroacetyl chloride, pyridine/diethyl ether, 0 °C to rt, 1 h, yield 67%; (q) acetic anhydride, pyridine, 0 °C to rt, 12 h, yield 70%; (r) AgO, acetone, rt, 72 h, yield 10%.

dx.doi.org/10.1021/ja402220t | J. Am. Chem. Soc. 2013, 135, 9777−9784

Table 1. Sequences and Properties of Cross-Linked Peptides

peptide	sequence[a]	λ_{max} (π–π^*) (nm)	λ_{max} (n–π^*) (nm)	cis $\tau_{1/2}$ (h)[d]
FK11	WGEACAREAAAREAACRQ	363	489	6
pAib	WGEACAABAABAABACRQ	367	474	13
Edbl-A	WGEACARAAAARAAACRQ	350	482	12
R10-A	WGEACAREAAAAEAACRQ	372	490	2.2
R5-A	WGEACAAEAAAREAACRQ	362	483	4.3
R5R10A	WGEACAAEAAAAEAACRQ	373	493	2.0
E-rich	WGEACAREAEAREAECRQ	366	491	7.2
A8-G	WGEACAREAGAREAACRQ	360	477	17
pG	WGEACAREGGGREAACRQ	359	471	27
JRK-7	EACARVBAACEAAARQ	359	470	–
SS-17[b]	WGACEAAAREAAAREAAARECAAQ	358	480	36
FK11[b]	WGEACAREAAAREAACRQ	357	479	45
FK11[c]	WGEACAREAAAREAACRQ	327	480	3.5
GSH	γECG (X2)	369	471	–

[a]"B" denotes an Aib residue; all peptides are N-acetylated and C-amidated. [b]Cross-linked with **3**. [c]Cross-linked with **4**. [d]Measured at 37 °C.

highly polar to nonpolar side products were produced, which we could not characterize. One could prepare **5-rf** via a diazonium coupling reaction sequence of four steps as used for **4-rf**, but the overall yield would appear to be less than 10%. In general, we obtain low yields for diazo coupling reactions of di-ortho-substituted donors and di-ortho-substituted acceptors, which we believe is due to steric hindrance caused by the ortho substituents. Higher yielding synthetic approaches to these types of compounds would be very useful.

Peptide Synthesis and Cross-Linking. The peptides listed in Table 1 were prepared using standard Fmoc-based solid-phase peptide synthesis methods and purified by reverse-phase HPLC on a semipreparative RX-C8 column (Zorbax, 9.4 mm ID × 255 mm) using a linear gradient of 10–65% acetonitrile/H_2O (containing 0.1% trifluoroacetic acid) over a course of 25 min. The molecular compositions of peptides were confirmed by ESI-MS [M^+].

The cross-linking reactions of peptides were generally carried out in 50% DMSO/water. A solution of 0.5 mM peptide (freshly purified by HPLC) and 2 mM cross-linker in 50 mM Tris buffer at pH 8 was stirred at 40 °C under a nitrogen gas atmosphere for 20 h. The progress of the reaction was monitored using MALDI mass spectrometry. The reaction was dried under high vacuum, and the cross-linked peptide was purified by HPLC (SB-C8 column, as described above) using a linear gradient of 10–70% acetonitrile/water (containing 0.1% trifluoroacetic acid) over the course of 25 min. The compositions of cross-linked peptides were confirmed by ESI-MS.

Microinjection into Zebrafish Embryos and Fluorescence Imaging in Vivo. Zebrafish embryos (*Danio rerio*, AB strain) were maintained at 28 °C and staged as described in Kimmel et al.:[27] 3 μL of each peptide: Fl-$(Pro)_9$-FK11) linked to **4** (in PBS, 1.0 mM), and the unlinked control peptide Fl-$(Pro)_9$-FK11) (in PBS, 1.3 mM) were backfilled into glass needles, and ∼3 nL of each were injected into the yolk of 1–2 cell-stage embryos (n > 25 for each group). Embryos were maintained in the dark. Images were captured with a Lumar V12 fluorescent stereomicroscope (Zeiss) with an Axiocam MRc digital camera and software. Development appeared normal as determined by comparing injected embryos to uninjected embryos at each stage (Figure S6 in Supporting Information [SI]). Fluorescence imaging and time courses were carried out on an Olympus IX71 microscope with a UPlanFL 10×/0.30 NA objective lens. The illumination source was a 103-W/2 short arc mercury lamp (3000 lm). Photoswitching was carried out at room temperature (∼23 °C). A fluorescein filter set (Omega Optical Inc. Alpha Vivid XF100-3, ex. 450–490 nm, em. 505–580 nm) was used for imaging the embryos and as the blue light source to trigger cis-to-trans isomerization. A customized Cy5 filter set with excitation filter (630AF50/25R (606–650 nm)) was used as the red light source to cause trans-to-cis isomerization. Exposure to ∼5 s of red light (nominally (out of focus) 60 mW/cm^2) was routinely used to produce the maximum amount of the cis isomer.

RESULTS AND DISCUSSION

Red-Light Photoswitching of 1. To explore the suitability of tetra-ortho-methoxy-substituted azobenzene derivatives for biomolecule photocontrol, we synthesized the thiol-reactive derivative **1** suitable for linking to peptide and protein targets. We used **1** to cross-link the helix-forming peptide FK11, which has Cys residues spaced i, i+11 in the sequence (Table 1). This peptide is well-established as a sequence where helix–coil transitions can be driven by cis–trans isomerization of azobenzene switches.[28]

Surprisingly, attachment to the peptide caused a red-shift in the absorbance of **1** relative to the reference compound **1-rf** in water (λ_{max} 490 vs 470 nm) (Figure 1a). While this λ_{max} is still a long way from the red region of the spectrum, the n–π^* band has a tail past 600 nm (Figure 1a). Moreover, if one plots the ratio of the absorbance of the trans and cis isomers of **1** linked to the FK11 peptide, it is seen that the trans isomer has a larger absorbance than the cis throughout the wavelength range 500–700 nm (Figure 1b). This behavior is not observed with common azobenzene photoswitches that do not have the tetra-ortho-substitution pattern. We therefore decided to irradiate the sample with red light (635 nm, 90 mW/cm^2) and found nearly complete (∼98%, based on comparison with the isolated cis isomer of **1-rf**)[17] conversion to the cis isomer (Figure 1a). As expected, trans-to-cis isomerization of the photoswitch also drove helical folding of the attached peptide (Figure 1c,d). We found that irradiation with 660 nm light of similar intensity (80 mW/cm^2) also produced trans-to-cis isomerization but at a slower rate consistent with a weaker absorbance of the photoswitch at longer wavelengths (Figure 1a). Because the thermal back reaction is slow ($\tau_{1/2}$ 6 h, Table 1) even a relatively slow rate of photochemical trans-to-cis isomerization produces the cis isomer at a competitive rate. Near-IR wavelengths (760 nm, 1 W/cm^2) however, proved ineffective in causing isomerization. The trans isomer can be regenerated (to ∼85%) rapidly with blue light (Figure S1 in SI).

From a biological applications standpoint, the importance of being able to drive isomerization with red rather than green light can be appreciated simply by shining a red vs a green laser pointer at one's hand; the absorption coefficients of oxygenated mammalian tissue differ by a factor of ∼100 between 635 nm (red) and 535 nm (green) wavelengths.[3] Red-light-driven isomerization thus makes optical manipulation of targets in higher organisms possible.

dx.doi.org/10.1021/ja402220t | J. Am. Chem. Soc. 2013, 135, 9777–9784

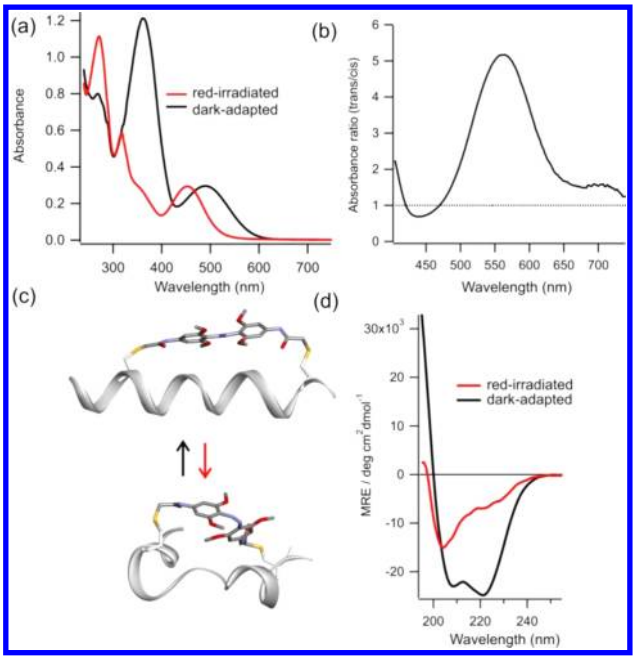

Figure 1. (a) UV−vis spectra of the peptide FK11 (WGEACAREAA-AREAACRQ) cross-linked with **1**. Dark-adapted (trans) spectra and red-light-irradiated (635 nm, 90 mW/cm^2 for 5 min or 660 nm, 80 mW/cm^2 for 25 min) spectra in 5 mM NaPi buffer pH 7.0, 20 °C. (b) Ratio of the absorbance of the dark-adapted cross-linked peptide to that of the red-light-irradiated sample (trans/cis) (c) Model of the FK11 peptide cross-linked with **1** in trans and cis states. (d) Circular dichroism (CD) spectra of **1**-cross-linked FK11 indicate a red-light-driven decrease in helix content.

Red-Light Photoswitching Occurs with a Variety of Peptides. Concerned that this result was due to a peculiarity of the interaction of **1** with the specific peptide sequence FK11, we made a series of analogues of the peptide that varied greatly in helical propensity and/or amino acid composition near the photoswitch attachment site (Table 1). The λ_{max} of the n−π* transition of the trans isomer varied significantly among these peptides (Table 1). However, all of these, even those with extremely weak absorbance in the red region of the spectrum, could be isomerized effectively with red light (Figure S1 in SI). Red-light-driven trans-to-cis isomerization resulted in a decrease in the α-helix content of the attached peptide in each case (Figure S2 in SI). As expected, the rate of trans-to-cis conversion with red light of a given intensity and a given wavelength depended on the molar extinction coefficient of the switch/target combination.

Factors Affecting the Position of the Absorption Bands. Time-dependent density functional theory calculations suggest that the red-shift of the n−π* band of the trans isomer arises due to a destabilization of the HOMO centered on the azo nitrogen lone pairs because of the close proximity of the methoxy oxygen lone pairs.[17] We propose that the variability of the position of the trans n−π* band among **1**-cross-linked peptides is due to variation in solvent H-bonding to the azo nitrogens and methoxy groups and concomitant alteration in the degree of coplanarity of the aromatic rings. This hypothesis is consistent with the finding that the position of the n−π* transition of the trans isomer of **1-rf** is temperature sensitive in water.[17]

A specific example of the effects of H-bonding on the absorption properties of a tetra-ortho-methoxy azobenzene compound was encountered during the preparation of derivatives of **1**. Two distinct crystal forms of para-bromo tetra-ortho-methoxy azobenzene (**2**) were isolated from a chloroform/methanol solution. In one form, the aromatic rings are highly twisted at an angle of 65° (Figure 2a). In the second

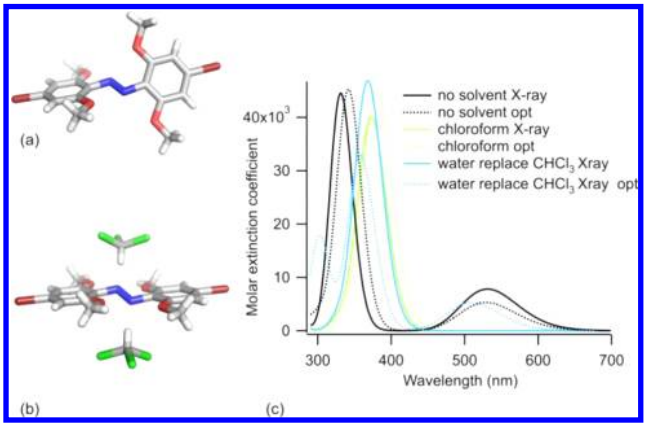

Figure 2. X-ray crystal structures of **2** without solvent (a) and with cocrystallized chloroform molecules (b). In the solvent-free form, the rings are highly twisted at an angle of 65°. In the second crystal form, the H atoms of each of two chloroform molecules interact with an azo nitrogen atom and oxygen atoms from two methoxy groups. These interactions result in a much more planar ring system. (c) Calculated (TD-DFT, B3LYP/6-311++G**) spectra of **2** based on the X-ray structures before and after optimization (opt). Only the nonplanar structures show long wavelength n−π* absorption bands.

form, the H atoms of each of two chloroform molecules H-bond with an azo nitrogen atom and oxygen atoms from two methoxy groups (Figure 2b). These interactions result in a nearly planar ring system. Time-dependent density functional theory calculations (B3LYP/6-311++G**) on each of these structures confirm large changes in the position of the n−π* (and π−π*) bands (Figure 2c), and indeed, the two crystal forms have distinct colors (orange, yellow).

The Generality of Red-Light Switching with Tetra-Ortho-Substituted Azo Compounds. To further test the generality of the tetramethoxy scaffold as a red-light switch, we synthesized the extended derivatives **3** and **3-rf** (Scheme 2). The trans isomer of compound **3** has an end-to-end distance of ∼20 Å, and this changes to ∼12 Å upon isomerization to cis.[29] Photocontrol of the structure of larger peptides and proteins is likely to be facilitated with longer rigid photoswitchable cross-linkers of this type.[30] The X-ray structure of the trans isomer of **3-rf** showed the compound was also nonplanar (Figure 3b). A red-shifted n−π* band and effective red-light driven trans-to-cis isomerization (93% cis) was observed with **3-rf** in solution (Figure 3a, Figures S3, S4 in SI). Attachment of photoswitch **3** to peptides with Cys residues spaced *i*, *i*+17 (trans) and *i*, *i*+ 1 (cis) was found to enable red-light-driven helix−coil transitions, either increasing or decreasing helix content, depending on the Cys spacing (Figure 3c,d, Figure S2 in SI).

We then tested whether oxygen substituents were strictly required by synthesizing ortho-chloro- and -bromo- derivatives (**4-rf**, **5-rf**) (Scheme 3). The chloro and bromo species also gave trans isomers with red-shifted n−π* transitions that could be effectively isomerized to the cis form with red light (Figures S3, S4 in SI). Cross-linking of the peptide FK11 with **4** again led to photocontrol of helix content upon red-light illumination (Figure 4). The result is therefore quite general.

dx.doi.org/10.1021/ja402220t | J. Am. Chem. Soc. 2013, 135, 9777−9784

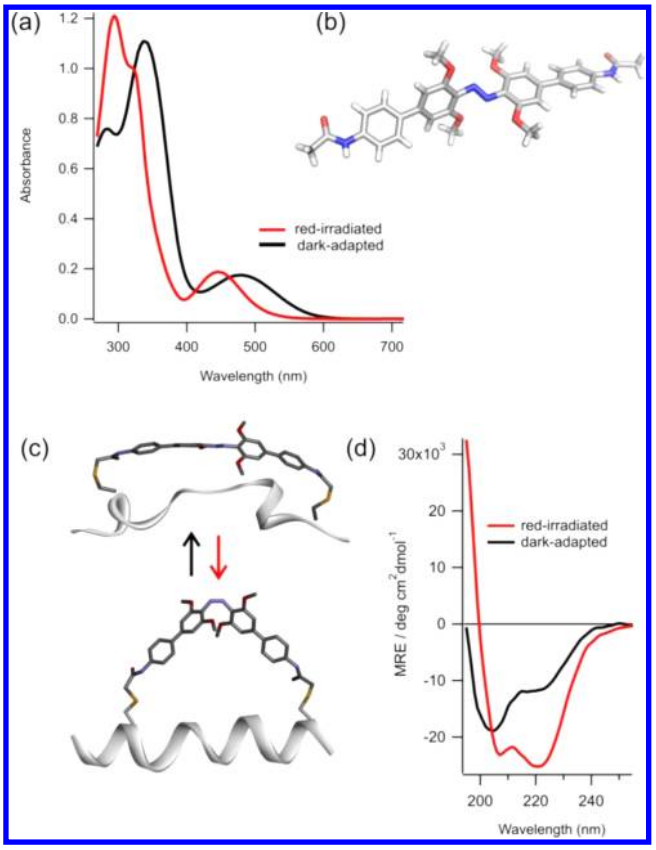

Figure 3. (a) UV−vis spectra of cross-linked with **3**. Dark-adapted (trans) spectra and red-light-irradiated (635 nm, 90 mW/cm^2 for 5 min) spectra in 5 mM NaPi buffer pH 7.0, 20 °C. (b) X-ray structure of trans **3-rf**. (c) Model of FK11 cross-linked with **3** in trans and cis states. (d) CD spectra of **3**-cross-linked FK11 showing a red-light-driven increase in helix content.

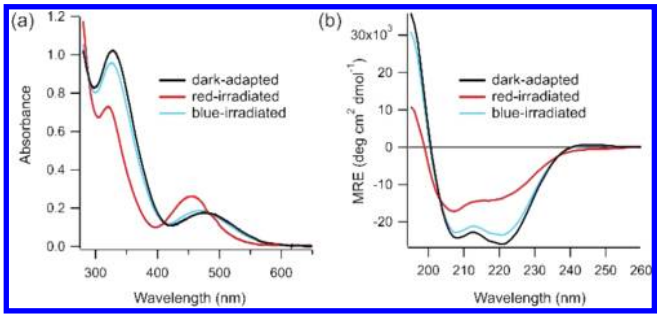

Figure 4. (a) UV−vis spectra and (b) CD spectra of compound **4** cross-linked to peptide FK11 (see Table 1 for sequence) under the indicated irradiation conditions in 10 mM sodium phosphate buffer, pH 7, 20 °C.

We did not synthesize the corresponding fluoro derivative since it was not predicted (B3LYP, 6-31G*) to show a large separation of n−π* bands. However, Hecht and colleagues have reported that, in fact, this derivative does show separation of the n−π* bands, particularly when an electron-withdrawing para-substituent is present.[24] It would be of significant interest to test if this compound, too, undergoes red-light switching. The trans isomer of the BF2-substituted azo compound reported by Aprahamian et al. has a higher extinction coefficient than the cis isomer at wavelengths greater than 600 nm and, thus, may also be expected to undergo red-light-driven isomerization. The surprising enhancement of the thermal relaxation rate reported for this compound in the presence of oxygen may complicate biological applications, however.[23]

Resistance to Reduction by Glutathione. A second concern besides the wavelength for photocontrol in vivo is the chemical and metabolic stability of the photoswitch. Azo compounds may undergo photobleaching, reduction by intracellular glutathione, or enzymatic metabolism. These processes depend critically on the specific structure of the azo compound and its redox potential.[13,31] The tetra-ortho-methoxy compounds **1** and **3** were found to be stable to photobleaching but underwent slow reduction ($\tau_{1/2} \approx 1$ h) in the presence of 10 mM reduced glutathione in their trans isomeric states (Figure S5 in SI). This sensitivity to reduction means that only extracellular use and short-term intracellular use are possible in vivo.

The tetra-ortho-chloro-substituted azobenzene compound **4**, however, proved resistant to reduction by glutathione in both isomeric forms (Figure 5) and was also stable to photo-

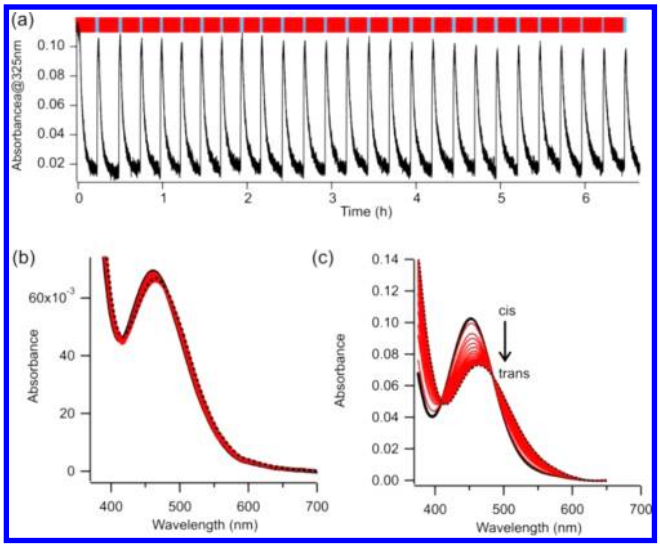

Figure 5. Stability to photobleaching and to reduction by glutathione of **4**-cross-linked FK11 (a) Multiple cycles of red-/blue-light switching in 10 mM phosphate buffer, pH 7. (b) Photoswitch **4**, in the trans state, cross-linked to FK11 was incubated in 10 mM reduced glutathione for 16 h at 25 °C. The first scan is shown as a solid black line. Intermediate scans are shown as red lines. The final scan is shown as a black dotted line. No change is evident. Normal red/blue light photoswitching (as in Figure 4) was observed after this incubation. (c) Photoswitch **4**, in the cis state, cross-linked to FK11 was incubated in 10 mM reduced glutathione for 16 h at 25 °C. Thermal cis-to-trans isomerization also occurs over this time period. Normal red-/blue-light photoswitching was observed after this incubation.

bleaching (Figure 5). This result was unexpected since chloro substituents are more electron-withdrawing than methoxy substituents and so might be expected to increase susceptibility to reduction. The nonplanar conformation of the trans isomer decreases the electron-donating ability of the methoxy groups via resonance, but the methoxy group is still less electron withdrawing than the chloro group via induction.[32]

The mechanism of reduction of azo compounds by thiols has been studied by Kosower and colleagues who determined that, for diazenedicarboxylic acid derivatives, the thiol attacks one azo nitrogen atom, and the second azo nitrogen atom becomes protonated to give a sulfenyl hydrazine derivative.[33]

dx.doi.org/10.1021/ja402220t | J. Am. Chem. Soc. 2013, 135, 9777−9784

The azo compounds studied here are more electron rich than the compounds studied by Kosower. We hypothesize that thiol attack in the present case is facilitated by prior, or concomitant, protonation of the azo group to enhance its electrophilicity. If this is the case, the enhanced rate of reduction of the tetra-ortho-methoxy compound by glutathione could be due to a higher effective pK_a of the azo group. We determined the ease of protonation of the tetra-ortho-methoxy (**1**)- and tetra-ortho-chloro (**4**)-substituted FK11 by measuring UV−vis spectra as a function of pH (panels a and b of Figure 6). These data confirm

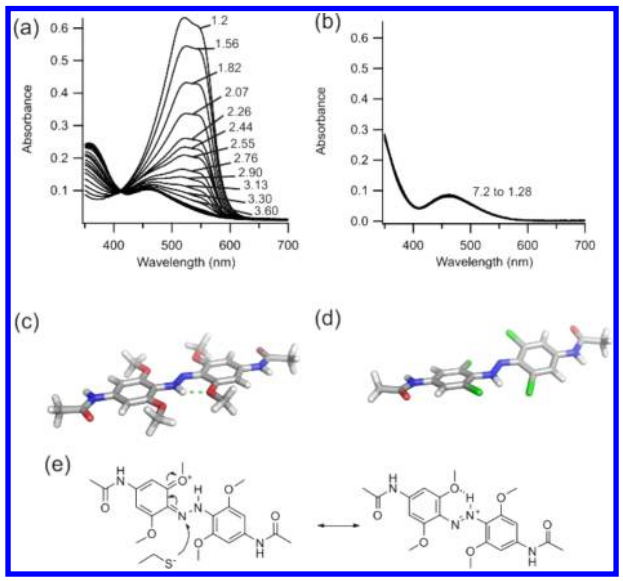

Figure 6. Protonation of the azo group of **1**-cross-linked FK11 (a) becomes significant below pH 4, whereas no protonation is evident for **4**-cross-linked FK11 even at pH 1.3. The pHs are indicated in the figure. (b). Calculated minimum energy structures (B3LYP/6-311++G**) of **1-rf** (c) and **4-rf** (d) indicate that protonation leads to a planar structure for **1-rf**. The protonated **1-rf** may be represented as shown in (e) and is expected to be attacked by thiols more easily than the unprotonated form.

that the tetra-ortho-methoxy species is more easily protonated than the tetra-ortho-chloro **4**-substituted FK11 peptide. The conformations of the protonated cross-linkers were determined using computational methods (B3LYP/6-311++G**) and are shown in panels c and d of Figure 6. The tetra-ortho-methoxy compound is planar, while the tetra-ortho-chloro species remains twisted. The planar conformation of the protonated tetra-ortho-methoxy compound again implicates H-bonding to the methoxy groups as playing an important role in the behavior of these compounds. Protonation of an azo nitrogen is expected to facilitate attack by thiols as shown in Figure 6e. This may occur prior to, or in concert with, nucleophilic attack.

Red-Light Photoswitching in Vivo. To examine the possibility of photoswitching with red light with photoswitch **4** directly in vivo, a fluorescent reporter sequence (fluorescein-[D]-PPPPPPPPPEACAREAAAREA-ACRQ; Fl-(Pro)$_9$-FK11) was designed. D-Amino acids were used to avoid degradation of the reporter peptide by proteases in vivo.[13] Fluorescein was chosen since its emission spectrum overlaps to different extents with the n−π* bands of the trans and cis isomers of **4**; thus, fluorescence should be quenched to different extents by the trans and cis isomers via fluorescence resonance energy transfer. Blue light was expected to excite fluorescein and simultaneously drive cis-to-trans isomerization of the photo-switch. Also, intense red light was expected to drive trans-to-cis isomerization without exciting (or bleaching) fluorescein.

Figure 7 shows models of the fluorescent reporter peptide cross-linked with **4**. A solution of the peptide was first irradiated

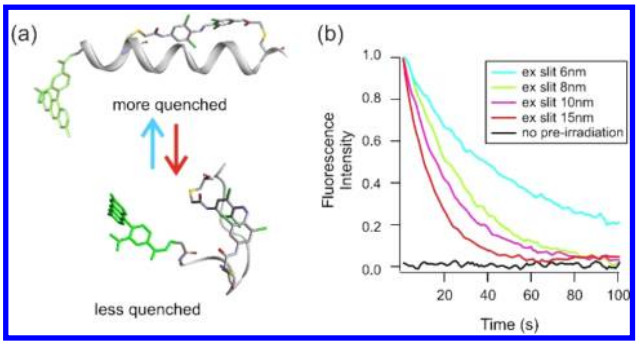

Figure 7. (a) Models of the fluorescent reporter peptide fluorescein-[D](Pro)$_9$-FK-11 cross-linked with **4** in the trans (blue irradiated and cis (red irradiated) states. The trans state results in greater quenching of fluorescein emission. (b) In vitro photoswitching in 20% DMSO in phosphate buffered saline. Samples were pre-irradiated with red light to convert them to the cis state. Samples were then irradiated with blue light (460 nm), and fluorescence emission at 520 nm was monitored as a function of time. Blue light excites fluorescein and simultaneously switches the azo group from cis to trans. As the blue light intensity was increased by increasing the excitation monochromator slit width (indicated), the rate of cis-to-trans isomerization increased. No fluorescence change was seen if the sample was not first converted to the cis isomer with red light (black trace).

with red light to convert the photoswitch to the cis isomeric state. The solution was then exposed to blue light, and the time course of fluorescence emission was monitored. As expected, blue light produced a time-dependent fluorescence decrease as it converted cis species into trans (Figure 7b). The rate of this process depended on the intensity of the blue-light source (which was varied by varying the excitation slit width in the fluorescence spectrophotometer in Figure 7b).

To test photoisomerization in vivo, the reporter peptide was microinjected into zebrafish embryos. The zebrafish provides a convenient model system for in vivo testing of photoswitchable peptides and proteins.[13] First, microinjection into the yolk at the yolk−cell interface during embryogenesis ensures the photoswitchable biomolecule is carried throughout the organism to all types of cells and tissues. Second, the optical transparency of the fish embryos enables convenient fluorescence monitoring of the photoswitch using a blue-light-absorbing/green-light-emitting dye, and finally, blue light can be used to reset the switch in order to rapidly test many cycles of photoswitching. Zebrafish embryos (n > 25 for each group) were injected at the 1−2 cell stage with the Fl-(Pro)$_9$-FK11 peptide cross-linked with **4** or an uncross-linked control peptide and subsequently imaged at 5.5 h post fertilization (hpf) or 24 hpf. In all cases, there was no evidence of gross morphological changes or delays in the rate of development, indicating no apparent peptide toxicity (Figure S6 in SI). Robust fluorescence changes confirming red-light/blue-light switching were seen at least until the early pharyngula period of development[27] (~30 h) (Figure 8a,b) The fluorescently labeled peptide fluorescein-(Pro)$_9$-FK11 lacking a photoswitch did not show any time-dependent emission, only a linear bleaching (Figure 8c,d).

dx.doi.org/10.1021/ja402220t | J. Am. Chem. Soc. 2013, 135, 9777−9784

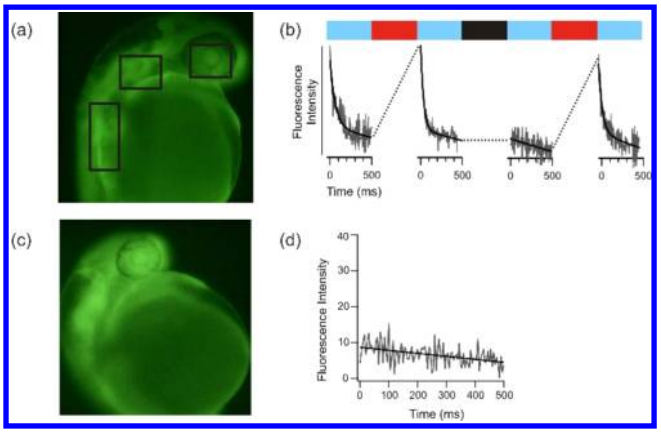

Figure 8. (a) Fluorescence image of a zebrafish embryo (early pharyngula stage/~30 hpf) containing the fluorescent reporter peptide fluorescein-[D](Pro)$_9$-FK-11 cross-linked with **4**. (b) Measurements of fluorescence intensity at the zones indicated by black boxes in (a), as a function of time during blue light irradiation. As was observed in vitro (Figure 7), a change in fluorescence emission was seen only if the peptide was first switched with red light (indicated by red bars). No pre-irradiation with red light (indicated by black bar) before blue light produces no exponential (switching) transient, only a background slope due to fluorescein reporter photobleaching. Note the blue light intensity is ~1000 fold higher here than in Figure 7. (c) Fluorescence image of a zebrafish embryo (~30 hpf) containing the fluorescent reporter peptide fluorescein-[D](Pro)$_9$-FK11 without a photoswitch. (d) Measurement of fluorescence intensity of the nonswitchable peptide as a function of time during blue-light irradiation after pre-irradiation with red light as in (b).

CONCLUSIONS

As a class, the tetra-ortho-substituted azobenzene compounds described here extend the versatility of azobenzene-based switches for in vivo use by providing the capability of conformational control using red light. Red light can effectively penetrate tissue in most organisms, and red-light-absorbing compounds can permit studies on whole living animals.[34,35] These red-light switchable azo compounds can be readily synthesized and derivatized for attachment to a wide variety of targets. Their small size combined with their robust and predictable conformational changes can be used to rationally design a wide range of light-driven molecular responses.

ASSOCIATED CONTENT

Supporting Information

Synthetic procedures, computational details, NMR data, further UV/vis and CD data, and crystallographic information files. This material is available free of charge via the Internet at http://pubs.acs.org.

AUTHOR INFORMATION

Corresponding Author

awoolley@chem.utoronto.ca

Author Contributions

[§]S.S. and A.A.B. contributed equally.

Notes

The authors declare no competing financial interest.

ACKNOWLEDGMENTS

This research has been supported by the Natural Sciences and Engineering Research Council of Canada and the National Institutes of Health (USA) (R01 MH086379)

REFERENCES

(1) *Molecular Switches*, 2nd ed.; Feringa, B., Browne, W. R., Eds.; Wiley-VCH: Weinheim, 2011.
(2) Wyart, C.; Del Bene, F.; Warp, E.; Scott, E. K.; Trauner, D.; Baier, H.; Isacoff, E. Y. *Nature* **2009**, *461*, 407−410.
(3) Wang, L. V.; Wu, H.-i. *Biomedical Optics: Principles and Imaging*; Wiley: New York, 2007.
(4) Fenno, L.; Yizhar, O.; Deisseroth, K. *Annu. Rev. Neurosci.* **2011**, *34*, 389−412.
(5) Levskaya, A.; Weiner, O. D.; Lim, W. A.; Voigt, C. A. *Nature* **2009**, *461*, 997−1001.
(6) Hartley, G. S. *Nature* **1937**, *140*, 281−281.
(7) Beharry, A. A.; Woolley, G. A. *Chem. Soc. Rev.* **2011**, *40*, 4422−4437.
(8) Yager, K. G.; Barrett, C. J. *J. Photochem. Photobiol., A* **2006**, *182*, 250−261.
(9) Hoppmann, C.; Schmieder, P.; Domaing, P.; Vogelreiter, G.; Eichhorst, J.; Wiesner, B.; Morano, I.; Ruck-Braun, K.; Beyermann, M. *Angew. Chem., Int. Ed.* **2011**, *50*, 7699−7702.
(10) Volgraf, M.; Gorostiza, P.; Numano, R.; Kramer, R. H.; Isacoff, E. Y.; Trauner, D. *Nat. Chem. Biol.* **2006**, *2*, 47−52.
(11) Polosukhina, A.; Litt, J.; Tochitsky, I.; Nemargut, J.; Sychev, Y.; De Kouchkovsky, I.; Huang, T.; Borges, K.; Trauner, D.; Van Gelder, R. N.; Kramer, R. H. *Neuron* **2012**, *75*, 271−282.
(12) Fehrentz, T.; Schonberger, M.; Trauner, D. *Angew. Chem., Int. Ed.* **2011**, *50*, 12156−12182.
(13) Beharry, A. A.; Wong, L.; Tropepe, V.; Woolley, G. A. *Angew. Chem., Int. Ed.* **2011**, *50*, 1325−1327.
(14) Zhang, F.; Timm, K. A.; Arndt, K. M.; Woolley, G. A. *Angew. Chem., Int. Ed.* **2010**, *49*, 3943−3946.
(15) Mourot, A.; Kienzler, M. A.; Banghart, M. R.; Fehrentz, T.; Huber, F. M.; Stein, M.; Kramer, R. H.; Trauner, D. *ACS Chem. Neurosci.* **2011**, *2*, 536−543.
(16) Wegner, H. A. *Angew. Chem., Int. Ed.* **2012**, *51*, 4787−4788.
(17) Beharry, A. A.; Sadovski, O.; Woolley, G. A. *J. Am. Chem. Soc.* **2011**, *133*, 19684−19687.
(18) Sadovski, O.; Beharry, A. A.; Zhang, F.; Woolley, G. A. *Angew. Chem., Int. Ed.* **2009**, *48*, 1484−6.
(19) Li, Y.; Patrick, B. O.; Dolphin, D. *J. Org. Chem.* **2009**, *74*, 5237−5243.
(20) Samanta, S.; Qin, C. G.; Lough, A. J.; Woolley, G. A. *Angew. Chem., Int. Ed.* **2012**, *51*, 6452−6455.
(21) Siewertsen, R.; Neumann, H.; Buchheim-Stehn, B.; Herges, R.; Nather, C.; Renth, F.; Temps, F. *J. Am. Chem. Soc.* **2009**, *131*, 15594−15595.
(22) Sell, H.; Nather, C.; Herges, R. *Beilstein J. Org. Chem.* **2013**, *9*, 1−7.
(23) Yang, Y.; Hughes, R. P.; Aprahamian, I. *J. Am. Chem. Soc.* **2012**, *134*, 15221−15224.
(24) Bleger, D.; Schwarz, J.; Brouwer, A. M.; Hecht, S. *J. Am. Chem. Soc.* **2012**, *134*, 20597−20600.
(25) Wepster, B. M. *Recl. Trav. Chim. Pays-Bas* **1954**, *73*, 809−818.
(26) Merino, E. *Chem. Soc. Rev.* **2010**, *40*, 3835−3853.
(27) Kimmel, C. B.; Ballard, W. W.; Kimmel, S. R.; Ullmann, B.; Schilling, T. F. *Dev. Dyn.* **1995**, *203*, 253−310.
(28) Ihalainen, J. A.; Paoli, B.; Muff, S.; Backus, E. H.; Bredenbeck, J.; Woolley, G. A.; Caflisch, A.; Hamm, P. *Proc. Natl. Acad. Sci. U.S.A.* **2008**, *105*, 9588−9593.
(29) Standaert, R. F.; Park, S. B. *J. Org. Chem.* **2006**, *71*, 7952−7966.
(30) Beharry, A. A.; Chen, T.; Al-Abdul-Wahid, M. S.; Samanta, S.; Davidov, K.; Sadovski, O.; Ali, A. M.; Chen, S. B.; Prosser, R. S.; Chan, H. S.; Woolley, G. A. *Biochemistry* **2012**, *51*, 6421−641.
(31) Levine, W. G. *Drug. Metab. Rev.* **1991**, *23*, 253−309.

(32) Ritchie, C. D.; Sager, W. F. *Prog. Phys. Org. Chem.* **1964**, *2*, 323−400.
(33) Kosower, E. M.; Kanety-Londner, H. *J. Am. Chem. Soc.* **1976**, *98*, 3001−3007.
(34) Ntziachristos, V. *Annu. Rev. Biomed. Eng.* **2006**, *8*, 1−33.
(35) Shcherbo, D.; Shemiakina, I. I.; Ryabova, A. V.; Luker, K. E.; Schmidt, B. T.; Souslova, E. A.; Gorodnicheva, T. V.; Strukova, L.; Shidlovskiy, K. M.; Britanova, O. V.; Zaraisky, A. G.; Lukyanov, K. A.; Loschenov, V. B.; Luker, G. D.; Chudakov, D. M. *Nat. Methods* **2010**, *7*, 827−829.

CANCER

High fat deals a low blow

Nature, published online 26 June 2013; doi:10.1038/nature12347

Senescent cells, or those that are no longer dividing, produce the senescence-associated secretory phenotype (SASP), marked by a cocktail of cytokines, chemokines and enzymes that has been linked to cancer risk in obesity. To understand the basis for this link, Yoshimoto *et al*. studied the impact of diet on cancer in mice and found that cancer-prone mice consuming a high-fat diet, but not a normal diet, developed hepatocellular carcinoma. The authors did find evidence of senescent cells in the liver, and mice lacking IL-1β, an upstream regulator of SASP induction, had smaller numbers and sizes of tumors compared to wild-type mice. As intestinal microbiota have been linked to obesity, the authors then demonstrated that antibiotic treatment led to decreased populations of senescent cells and carcinoma. The authors searched for a possible mediator of this interaction, identifying a single molecule—deoxycholic acid—as highly present in the serum metabolites of mice fed with high-fat but not a normal diet. Decreasing deoxycholic acid concentrations blocked formation of carcinomas and senescent cells, and, reciprocally, treatment with this molecule increased cancer formation in mice on a high-fat diet. These data led to a model where high fat consumption initiates deoxycholic acid production, which induces formation of senescent cells, with subsequent SASP inducing cancer. *CG*

BIOSYNTHESIS

Deciphering dehydrophos

Proc. Natl. Acad. Sci. USA, published online 17 June 2013; doi:10.1073/pnas.1303568110

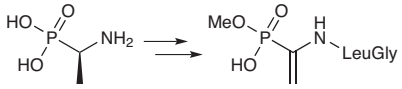

Dehydrophos is a broad-spectrum antibiotic produced by *Streptomyces luridus* that contains an aminophosphonate analog of dehydroalanine (ΔAla(P)). Cleavage of this phosphonotripeptide natural product by cellular peptidases releases methyl acetylphosphonate, which is a potent inhibitor of pyruvate dehydrogenase. Bougioukou *et al.* now report that the previously proposed mechanism for dehydrophos biosynthesis is incorrect. Analysis of the biosynthetic gene cluster suggested that it contains two putative 2-oxoglutarate/Fe(II)-dependent oxygenases, two putative alcohol dehydrogenases, two pyridoxal 5′-phosphate–dependent enzymes and two putative nonribosomal peptidyl transferases. The authors reconstituted and biochemically characterized several of these enzymes, and their experiments led them to propose a revised biosynthetic pathway with three phases. The first steps involve the formation of the C-P bond, a decarboxylation reaction and the reduction of phosphonoacetaldehyde to 2-hydroxyethylphosphonate, enzymatic reactions that have been observed in the biosynthetic pathways of other phosphonates. In the second part of the biosynthetic pathway, several enzymes convert 2-hydroxyethylphosphonate to L-Ala(P). The final phase involves two amide bond–forming reactions, monomethylation of the terminal phosphonic acid and the conversion of the C-C single bond adjacent to the phosphonate to a C-C double bond. Additional work is needed to uncover exactly how these enzymes efficiently catalyze such unusual biochemical transformations. *JMF*

PHOTOSWITCHES

Ready for red

J. Chem. Am. Soc., published online 10 June 2013; doi:10.1021/ja402220t

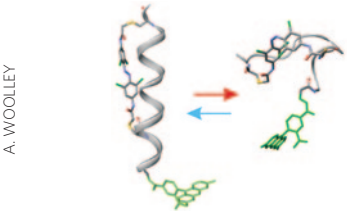

A. WOOLLEY

Photochemical tools allow scientists to use light to control the on and off state of a molecule. For *in vivo* application of these tools, switchable compounds must be responsive to red light; this requirement has limited applications of the popular azobenzene scaffold, for which no red light–activated derivatives are known. Samanta *et al.* now report a series of red light–activated azobenzenes and demonstrate their photoswitching properties *in vivo*. The authors showed that tetra-*ortho*-methoxy–substituted azobenzene can drive helix-to-coil transitions in FK-11, a peptide known to switch between conformations in response to isomerization of azobenzenes, and in other peptides in response to red light *in vitro*. In cells, azobenzene derivatives are also subject to reduction by glutathione, and the tetra-*ortho*-methoxy azobenzenes suffered from this weakness. The authors identified a tetra-*ortho*-chloro azobenzene that underwent stable *cis-trans* isomerization in response to red light and was resistant to reduction by glutathione. When linked to a fluorescent reporter peptide, this azobenzene yielded red light–mediated photocontrol in zebrafish embryos. Although it remains to be shown that these tools can be applied to interrogate a biological system *in vivo*, the development of red light–dependent, glutathione-resistant photochemical tools that can be readily derivatized makes these experiments possible. *AD*

NEUROSCIENCE

Along came a long RNA

Nat. Neurosci., published online 23 June 2013; doi:10.1038/nn.3438

The mechanisms underlying neuropathic pain include abnormal spontaneous activity in neurons of the dorsal root ganglion (DRG). Upon peripheral nerve injury, the expression of voltage-dependent potassium (Kv) channels is downregulated in the injured DRG neurons, which may help induce neuropathic pain. To understand the mechanism by which Kv channel downregulation contributes to development of pain, Zhao *et al.* asked whether long noncoding RNAs (lncRNAs), whose expression has recently been associated with disease, were at play. Searching a database of expressed sequence tags, the authors found one that represented the antisense sequence of the Kv1.2 channel transcript. This lncRNA was expressed in rat DRG neurons, with expressing neurons showing small amounts of Kv1.2 protein. Two types of nerve injury downregulated Kv1.2 mRNA and protein but upregulated the levels of lncRNA in the injured DRG neurons. This upregulation was attributed to nerve injury–induced increases in the expression of the transcriptional activator MZF1 and its binding to the promoter region of the lncRNA. Upregulating lncRNA downregulated Kv1.2 expression, reduced total Kv current and excitability in DRG neurons and produced neuropathic pain symptoms. Blocking nerve injury–induced increase in DRG lncRNA expression rescued nerve injury–evoked downregulation of DRG Kv1.2 and attenuated neuropathic pain. This discovery suggests that lncRNAs are potential targets in prevention and/or treatment of neuropathic pain. *MB*

Written by Mirella Bucci, Amy Donner, Joshua M. Finkelstein, Catherine Goodman & Terry L. Sheppard